

## SUPPLEMENTAL MATERIAL

### **Circadian gene variants and the skeletal muscle circadian clock contribute to the evolutionary divergence in longevity across *Drosophila* populations**

Liam C. Hunt, Jianqin Jiao, Yong-Dong Wang, David Finkelstein, Deepti Rao, Michelle Curley, Maricela Robles-Murguia, Abbas Shirinifard, Vishwajeeth R. Pagala, Junmin Peng, Yiping Fan, and Fabio Demontis

## SUPPLEMENTAL METHODS

### **Assays for muscle function (flight, negative geotaxis, jumping, and spontaneous locomotion)**

For flight assays, male flies of the specified ages were released into a “Sparrow chamber”, a plexiglass box that is 43-cm high, 27.5-cm wide, and 43-cm long, with a small opening to introduce the flies and having a light source at the top (Drummond et al. 1991). Flight tests were performed by releasing each fly to the center of the box and then scoring its ability to fly. Flies that flew upwards (U) were categorized as “good flyers” (index score 6), while those that flew horizontally (H) categorized as “moderate flyers” (index score 4), those that flew downwards (D) were categorized as “poor flyers” (index score 2), and those that fell and did not fly categorized as “non-flyers” (N; index score 0). Flight index is determined by using the formula  $6 (U) + 4 (H) + 2 (D) + 0 (N) / n$ , where n is the total number of flies for each line.

Negative geotaxis assays (climbing ability) were assessed every 8 days during lifespan measurements as described previously (Demontis and Perrimon 2010).

Jumping abilities were assessed by clipping wings with vannas scissors one day before the assay. On the day of the assay, flies were perched on top of 10-cm vial surrounded by a paper mat with concentric circles marked at every centimeter. The flies were persuaded with a paintbrush to jump from the edge of the vial onto the paper. For each fly, the average distance jumped was recorded from three attempts and normalized to that of young control flies (Wells et al. 1996).

For monitoring the spontaneous locomotion of flies, the TriKinetics system (#LAM-25H3 and #PSIU-9; [www.trikinetics.com](http://www.trikinetics.com)) was used according to manufacturer instructions, as previously done (Katewa et al. 2012). Spontaneous activity of groups of 10 flies/tube was recorded every 10 minutes under 12:12 hours dark:light cycles at 25°C.

### **Survival analysis**

For survival analysis, dead flies were counted every 2 days and the food was changed. To avoid any contribution of genetic background mutations to the observed lifespan phenotypes, similar procedures as before (Demontis et al. 2014) were followed. Specifically, *UAS-timeless* was backcrossed through more than six generations against  $y^1w^{1118}$  to obtain isogenic male siblings carrying either a *UAS-* or no transgene (distinguished by eye color: *white+* and *white-*,

respectively). Male siblings carrying either a *UAS*- or no transgene and having the same genetic background were then crossed to homozygous *w<sup>1118</sup>;Mhc-Gal4* (*rosy+ white-*) females and the resulting male progenies were sorted (based on eye color) into isogenic transgene-expressing and transgene-nonexpressing cohorts before lifespan analysis. *UAS*- transgene expression obtained with *Mhc-Gal4* was confirmed by qRT-PCR from fly thoraces, which consist mostly of skeletal muscle. Heterozygous *UAS*- transgene-alone controls were also analyzed to exclude that the observed phenotypes are due to differences in the genetic background. These flies were obtained by crossing *UAS*- males with female *w<sup>1118</sup>* virgins isogenic to the *w<sup>1118</sup>;Mhc-Gal4* stock.

To rule out any variation due to cytoplasmic background effects, all crosses were set up with female virgins from the *w<sup>1118</sup>;Mhc-Gal4* and *w<sup>1118</sup>* stocks. *UAS-mCherry* was used as alternative control. All the progenies analyzed consisted of males.

The *Ets21C* mutant (Bloomington stock number #18678) consists of a piggyBac insertion into the coding region of *Ets21C* which leads to loss of expression, as estimated with qRT-PCR for an amplicon downstream of the piggyBac insertion (Supplemental Fig. S1). The *Ets21C* mutant was backcrossed for 5 generations and isogenic wild-type controls and *Ets21C* heterozygous and homozygous mutant flies (distinguished by eye color) were compared in lifespan experiments.

### **Confocal image analysis**

Machine learning methods implemented in Fiji (Schindelin et al. 2012; Arganda-Carreras et al. 2017) were used to train three classifiers to segment protein aggregates imaged in the Ref(2)P/p62 and poly-ubiquitin channels, and regions representing muscle fibers in the phalloidin (F-actin) channel. Segmented muscle fiber images were used as masks to remove fluorescent signals outside the muscle fiber regions. Subsequently, the number and total area occupied by protein aggregates were determined in each image and normalized by the total area of muscle fibers in the same image.

### **Size analysis of indirect flight skeletal muscles**

Flies were snap frozen on glass slides with a drop of OCT in liquid nitrogen and bisected transversely in the middle of the thorax. Thorax sections were immediately fixed in 4% PFA for 30 minutes and washed three times with PBS. They were then incubated with AlexaFluor488-conjugated wheat-germ agglutinin (1:200) and AlexaFluor633-conjugated phalloidin (1:200) in PBS overnight at 4°C with rocking. The samples were then washed three times with PBS and

mounted on glass slides with polyvinyl alcohol mounting media with DABCO (Sigma-Aldrich #10981) and allowed to set at room temperature overnight. The slides were then imaged on a Nikon C2 confocal microscope and images analyzed using the Nikon Elements software for measuring the total cross-sectional area of all the 12 longitudinal indirect flight muscles considered together.

### **Proteome profiling by TMT-LC/LC-MS/MS**

The analysis was performed essentially following our previously optimized method (Bai et al. 2017). *Drosophila* thoraces, consisting mostly of skeletal muscle, from >50 male flies/replicate were lysed by a denaturing 8M urea-based buffer. Specifically, ~20 mg of tissue was lysed with ~400  $\mu$ L of the lysis buffer in a NextAdvance bullet blender at 4°C, with addition of ~200  $\mu$ L of glass beads. The lysate was further centrifuged to remove any remaining cuticle fragments. Protein concentration was determined in the resulting supernatant by a previously described short gel-based staining method (Xu et al. 2009). Three biological replicates were used for each genotype at each time point (1 week and 6 weeks).

Each sample was digested and desalted, followed by TMT labeling. The labeled samples were equally mixed and fractionated by basic pH reverse phase liquid chromatography (LC). The LC fractions were collected and further analyzed by acidic pH reverse phase LC-MS/MS. During ion fragmentation, the TMT reagents were cleaved to produce reporter ions for quantification. The collected raw MS data was searched against a database to identify peptides using a hybrid search engine (Wang et al. 2014). While the peptides were identified by MS/MS, the quantification was achieved by the fragmented reporter ions in the same MS/MS scans. The peptide quantification data were then corrected for mixing errors, and summarized to derive protein quantification results. Statistical analysis (ANOVA) was performed to determine cutoff for altered proteins (Niu et al. 2017).

### **Western blots for detergent-soluble and -insoluble fractions**

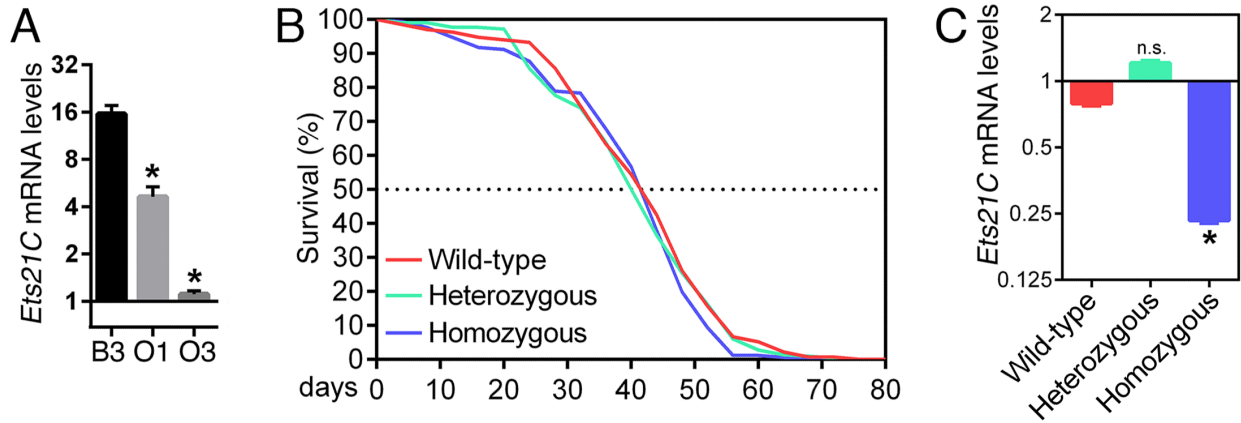
Western blots for detergent-soluble and insoluble fractions were done as before (Demontis and Perrimon 2010). In brief, thoraces were dissected from 20 male flies/sample and homogenized in ice-cold PBS with 1% Triton X-100 containing protease and phosphatase inhibitors. Homogenates were centrifuged at 14,000 rpm at 4°C and supernatants collected (Triton X-100 soluble fraction).

The remaining pellet was washed in ice-cold PBS with 1% Triton X-100. The pellet was then resuspended in RIPA buffer containing 8M urea and 5% SDS, centrifuged at 14,000 rpm at 4°C. The supernatants (Triton X-100 insoluble fraction) were collected and analyzed on 4-20% SDS-PAGE with anti-ubiquitin (Cell Signaling Technologies P4D1, #3936) and anti-Ref(2)P/p62 (Abcam #178840) antibodies.

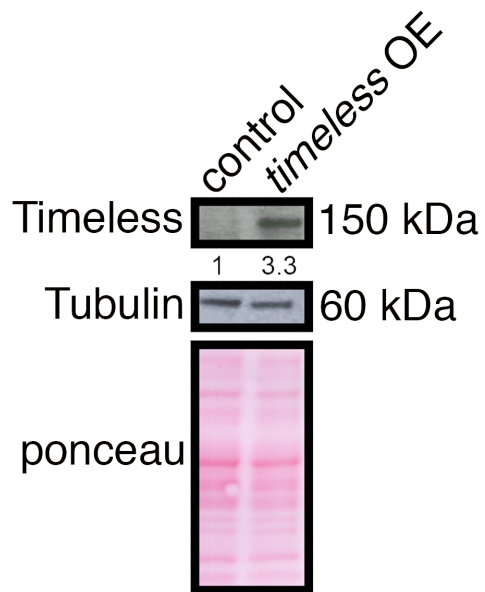
## SUPPLEMENTAL REFERENCES

- Arganda-Carreras I, Kaynig V, Rueden C, Eliceiri KW, Schindelin J, Cardona A, Sebastian Seung H. 2017. Trainable Weka Segmentation: a machine learning tool for microscopy pixel classification. *Bioinformatics* **33**: 2424-2426.
- Bai B, Tan H, Pagala VR, High AA, Ichhaporia VP, Hendershot L, Peng J. 2017. Deep Profiling of Proteome and Phosphoproteome by Isobaric Labeling, Extensive Liquid Chromatography, and Mass Spectrometry. *Methods Enzymol* **585**: 377-395.
- Demontis F, Patel VK, Swindell WR, Perrimon N. 2014. Intertissue control of the nucleolus via a myokine-dependent longevity pathway. *Cell reports* **7**: 1481-1494.
- Demontis F, Perrimon N. 2010. FOXO/4E-BP signaling in Drosophila muscles regulates organism-wide proteostasis during aging. *Cell* **143**: 813-825.
- Drummond DR, Hennessey ES, Sparrow JC. 1991. Characterisation of missense mutations in the Act88F gene of Drosophila melanogaster. *Mol Gen Genet* **226**: 70-80.
- Katewa SD, Demontis F, Kolipinski M, Hubbard A, Gill MS, Perrimon N, Melov S, Kapahi P. 2012. Intramyocellular fatty-acid metabolism plays a critical role in mediating responses to dietary restriction in Drosophila melanogaster. *Cell Metab* **16**: 97-103.
- Niu M, Cho JH, Kodali K, Pagala V, High AA, Wang H, Wu Z, Li Y, Bi W, Zhang H et al. 2017. Extensive Peptide Fractionation and y1 Ion-Based Interference Detection Method for Enabling Accurate Quantification by Isobaric Labeling and Mass Spectrometry. *Anal Chem* **89**: 2956-2963.
- Schindelin J, Arganda-Carreras I, Frise E, Kaynig V, Longair M, Pietzsch T, Preibisch S, Rueden C, Saalfeld S, Schmid B et al. 2012. Fiji: an open-source platform for biological-image analysis. *Nat Methods* **9**: 676-682.
- Wang X, Li Y, Wu Z, Wang H, Tan H, Peng J. 2014. JUMP: a tag-based database search tool for peptide identification with high sensitivity and accuracy. *Molecular & cellular proteomics : MCP* **13**: 3663-3673.
- Wells L, Edwards KA, Bernstein SI. 1996. Myosin heavy chain isoforms regulate muscle function but not myofibril assembly. *EMBO J* **15**: 4454-4459.
- Xu P, Duong DM, Peng J. 2009. Systematical optimization of reverse-phase chromatography for shotgun proteomics. *J Proteome Res* **8**: 3944-3950.

**SUPPLEMENTAL FIGURES AND FIGURE LEGENDS**



**Supplemental Figure S1.** *Ets21C* expression is upregulated in the B3 line but *Ets21C* null mutations do not extend lifespan. (A) Lower *Ets21C* mRNA levels are found in O1 and O3 lines compared with the parental B3 strain. SD with n=3 is shown, \* $p < 0.05$ . (B) Homozygous male *Ets21C* null flies (n=171) live similar to *Ets21C* heterozygous mutants (n=216) and to isogenic wild-type controls (n=134). (C) qRT-PCR analysis demonstrates that there is a reduction in *Ets21C* mRNA levels in homozygous male *Ets21C* null flies but not in wild-type and *Ets21C* heterozygous flies. SD with n=3, \* $p < 0.05$ .



**Supplemental Figure S2.** Validation of anti-Timeless antibodies via western blot. Compared to control samples, a band of the expected molecular weight for Timeless protein (~150 kDa) has increased intensity (~3.3-fold change) upon *timeless* overexpression (OE) in skeletal muscle, indicating that this band is specific.